

Cascaded active regions in 2.4 μm GaInAsSb light-emitting diodes for improved current efficiency

J. P. Prineas,^{a)} J. T. Olesberg, J. R. Yager, C. Cao, C. Coretsopoulos, and M. H. M. Reddy
Department of Physics and Astronomy, University of Iowa, Iowa City, Iowa 52242 and Optical Science and Technology Center, University of Iowa, Iowa City, Iowa 52242

(Received 24 July 2006; accepted 13 October 2006; published online 21 November 2006)

By cascading multiple GaInAsSb active regions, the authors have fabricated 2.4 μm light-emitting diodes that, for a given light output, operate at reduced current and higher voltage, which can be advantageous for battery-powered sensor applications. Tunnel heterojunctions separating emission regions add no measurable series resistance. Devices are demonstrated at room temperature with continuous wave output. © 2006 American Institute of Physics. [DOI: 10.1063/1.2392993]

The combination wavelength range (2.0–2.5 μm) is a key region of the electromagnetic spectrum for the measurement of biomolecules in aqueous samples due to vibrational transitions that provide unique absorption spectra.^{1,2} In the quest for compact optical sensors for medical applications such as continuous glucose sensing, there is a need for development of both sensitive photodetectors^{3,4} and broadband light sources^{5,6} (in order to cover the broad absorption resonances, typically tens of nanometers, of biomolecules in an aqueous environment) in this region. The quaternary alloy GaInAsSb is a promising material system for these applications with an energy gap that can be tuned across the 2.0–2.5 μm range while keeping the lattice constant matched to GaSb substrates. The last decade has seen the development of bright quaternary light emitting diodes (LEDs) operating at room temperature covering this spectral region.^{7,8}

LEDs are an ideal light source for many portable sensor applications because of their relatively high efficiency, high brightness (per unit frequency), broadband spectrum (typically $>2k_B T$ or 250 nm at room temperature), and compact size. By comparison, thermal sources can be compact and have larger bandwidth (>1000 nm), but are neither as efficient nor as bright. Diode lasers can have higher efficiency and brightness, but have spectrally narrow emission (~ 1 nm). Diode lasers can potentially be tuned across the combination wavelength range by using an external cavity,⁶ but this adds both size, complexity, and power draw, all detrimental for portable, battery powered sensors.

A potential inefficiency with single stage LEDs with peak emission near 2.4 μm is that they require small voltages to operate (~ 0.6 V), whereas analog and digital control electronics require 3.3 or 5 V. This voltage mismatch necessitates either separate battery sources for the LED and the control electronics, dc-dc converter components, or the use of a series resistor for reducing the voltage applied to the LED. The use of a series resistor leads to a waste of more than 80% of the power delivered to the LED, which can be the largest power draw in the system.

A more efficient alternative is to cascade multiple LED emitter regions epitaxially using tunnel junctions between stages. Figure 1 shows a real space band edge diagram of two quaternary emitting regions separated by a n^{++}/p^{++}

tunnel junction. An electron entering from the n side of the diode recombines with a hole and emits a photon in the first quaternary region, tunnels to the next region, and emits a second photon. For N cascaded active regions, the electron is recycled N times, so the operating current is reduced by a factor of N . The total efficiency, however, is unchanged, because the operating voltage increases by a factor N . The advantage of cascading is that the operating voltage can be matched to the battery voltage without the need for a dc-dc converter or the power waste of a series resistor. In addition, the current draw is reduced by a factor of N , which will extend battery life.

Cascaded active regions separated by low-resistance tunnel junctions in bipolar devices have been explored in the near infrared for high power applications^{9,10} in the context of reducing the series resistance of monolithic laser diode stacks, and at optical wavelengths,¹¹ communication wavelengths,¹² and near 2 μm (Ref. 13) for improved current efficiency. Cascading has also been proposed¹⁴ and demonstrated in interband midinfrared (3–5 μm) cascade lasers based on type II transitions in AlSb/InAs/GaSb quantum wells at low¹⁵ and room temperatures.¹⁶ In this letter, we demonstrate interband cascading in LEDs made from GaInAsSb quaternary semiconductors operating in the important combination wavelength range with continuous wave output at room temperature.

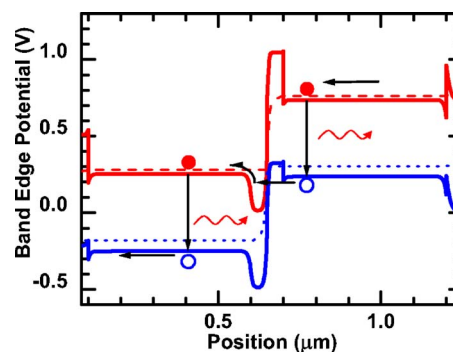


FIG. 1. (Color online) Real space band edge diagram of two GaInAsSb active regions separated by a n^{++}/p^{++} GaInAsSb/GaSb tunnel heterojunction, with the device forward biased to 0.95 V. Solid lines (red, blue) indicate the conduction and valence band (respectively), while (red) dashed and (blue) dotted lines indicate electron and hole Fermi levels, respectively. Arrows indicate how an electron (red solid circle) entering from the n side would cascade through the structure, combining with a hole (blue hollow circle) in each emission region.

^{a)}Electronic mail: john-prineas@uiowa.edu

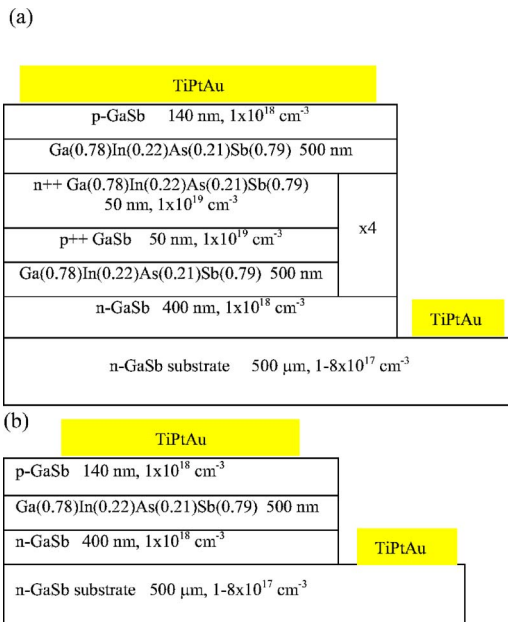


FIG. 2. (Color online) Heterostructure design for (a) the cascaded (ia1471) and (b) the single stage (ia1468) light-emitting diode.

For this study, we compare the performance of a single-stage and a five-stage LED. Heterostructure designs are shown in Fig. 2. The single stage device consisted of a $0.5 \mu\text{m}$ unintentionally doped layer of $\text{Ga}_{0.78}\text{In}_{0.22}\text{As}_{0.21}\text{Sb}_{0.79}$ clad by p - and n -doped GaSb layers for confinement of electrons, and grown on a GaSb substrate. Although the valence band of GaSb lies above that of the quaternary alloy, hole confinement can still be provided because of the n doping of the GaSb layer. Alternatively, holes can be confined if an AlGaAsSb cladding is used. Studies have shown improvements in LED performance ($\sim 50\%$ increased output at high current densities) for AlGaAsSb clads versus GaSb clads.¹⁷ We chose GaSb clads to keep the structures Al-free—Al is known to oxidize and reduce device lifetime—and for simpler growth—only one quaternary alloy needs to be calibrated rather than two.

The cascaded structure is composed of identical GaSb clads around the active region, which contains five $0.5 \mu\text{m}$ $\text{Ga}_{0.78}\text{In}_{0.22}\text{As}_{0.21}\text{Sb}_{0.79}$ layers separated by tunnel junctions. The tunnel junctions consist of a $n++/p++$ $\text{Ga}_{0.78}\text{In}_{0.22}\text{As}_{0.21}\text{Sb}_{0.79}/\text{GaSb}$ heterojunction with layer thicknesses of 50/50 nm. The real space band edge diagram of a single tunnel junction separated by two active regions is shown schematically in Fig. 1, with the device forward biased to 0.95 V. The heavy doping of both layers ensures a thin tunneling region. Additionally, the heavy n doping of the GaInAsSb layer moves the valence band to lower energy and blocks hole leakage from the left to the right emitting region. GaSb rather than GaInAsSb was needed in addition to heavy doping of the p layer in order to additionally raise the height of the electron barrier and prevent leakage of conduction band electrons from the right to the left emitting region.

Structures were grown by a molecular beam epitaxy (MBE) system equipped with valved crackers for group V elements yielding monomeric Sb and As_2 . Device structures were grown on n -type, (100)-oriented GaSb substrates $\sim 500 \mu\text{m}$ thick at a substrate temperature of 480°C , just above stoichiometric conditions (group V/III beam-equivalent-pressure flux ratio of ~ 1.6) as determined

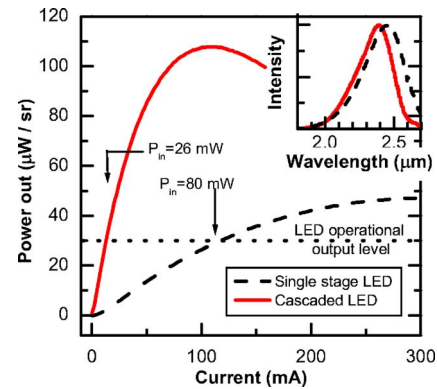


FIG. 3. (Color online) L - I curves recorded at room temperature for $200 \mu\text{m}$ square mesa single stage (black, dashed) and cascaded (red, solid) light-emitting diodes. The horizontal dotted line shows the nominal device operational output level. The inset shows spectrally resolved electroluminescence from the devices at the operational output level.

by reflection high energy electron diffraction oscillations. Based on the measured band gap ($2.5 \mu\text{m}$ cutoff wavelength from electroluminescence measurements) and the lattice constant (lattice mismatch to GaSb 1.8×10^{-3} as determined by high resolution x-ray diffraction measurements), the quaternary alloy composition is estimated to be $\text{Ga}_{0.78}\text{In}_{0.22}\text{As}_{0.21}\text{Sb}_{0.79}$.¹⁸ Be and GaTe were used for the p and n dopants, respectively.

The MBE grown wafers were processed into $200 \mu\text{m}$ square mesas using wet chemical etching to a depth just beyond the total thickness of the device structure into the substrate. After etching, TiPtAu was deposited on the mesa tops (p contact) and on the area surrounding the mesas (n contact) using a single evaporation. Electrical testing was performed using a probe station and a Hewlett-Packard 4155A parameter analyzer. Optical measurements were performed by placing the devices substrate side down on a glass window and electrically connecting to the back contacts with a probe station. Light emission was collected in a back-emission geometry (i.e., through substrate and glass) using an uncooled $2.6 \mu\text{m}$ extended-wavelength InGaAs detector, integrating output over a cone of solid angle of 0.037 sr. No antireflective coatings or condensing optics were used. Free carrier absorption by the n -GaSb substrate is not significant in the 2.0 – $2.5 \mu\text{m}$ wavelength range.⁴ All measurements were performed with continuous-wave operation at room temperature.

Figure 3 shows a comparison of the L - I characteristics of $200 \mu\text{m}$ square mesa diodes for the single stage and cascaded LEDs. To obtain an output power of $30 \mu\text{W}/\text{sr}$, the single-stage device requires 114 mA ($285 \text{ A}/\text{cm}^2$). The cascaded structure requires only 13 mA ($32 \text{ A}/\text{cm}^2$), which is a factor of nine times lower. The corresponding operating voltages, as can be seen from the I - V curves of the two devices in Fig. 4, are 0.7 V for the single stage LED and 2.1 V for the cascaded LED, which is a factor of three higher. The scaling of the current-voltage characteristics of the devices are comparable to, but deviate somewhat from the ideal factor of 5 expected for a five-stage cascaded device. The deviations likely stem from differences in device efficiencies.

From the observed scaling, it is clear the single stage LED (operating input power of 80 mW) is less efficient than the cascaded LED (operating input power 26 mW). We speculate that the thickness of the p -GaSb clad in these de-

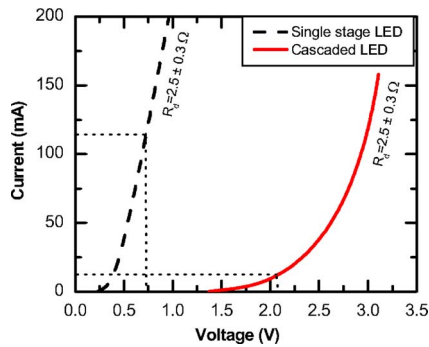


FIG. 4. (Color online) I - V curves recorded at room temperature for $200 \times 200 \mu\text{m}^2$ mesa single stage (black, dashed) and cascaded (red, solid) light-emitting diodes. Dotted lines indicate the operating voltage and current for the light-emitting diodes at the nominal operational output level.

vices is too thin, which would allow electrons to leak from the final stage of the active region to the semiconductor surface and the anode contact, decreasing radiative efficiency and increasing device heating. The lower efficiency of the single stage device means greater input power (voltage and current) are required to get the same output power.

The total upper hemisphere output of the LEDs can be estimated from Fig. 3. For a Lambertian angular dependence to the LEDs, which we confirmed with independent measurements, the total upper hemisphere output powers are 150 and $350 \mu\text{W}$ for the single stage and the cascaded LEDs. The total internal efficiency of the LEDs can also be estimated from Fig. 3,

$$\eta_{\text{internal}} = \frac{P}{TI \Delta\Omega_{\text{int}}} \frac{e}{E_{\text{photon}}} 100\%,$$

where P is the measured power emitted into the external solid angle $\Delta\Omega_{\text{ext}}$, with $\Delta\Omega_{\text{int}} [\approx \Delta\Omega_{\text{ext}}(n_{\text{ext}}/n_{\text{int}})^2]$ the corresponding internal solid angle, for current I into the device, T is the Fresnel transmission at the air/sample interface, e is electron charge, and E_{photon} is the photon energy. This equation assumes, conservatively, that all front-emitted light is reflected from the top solid contact into the back-emitting direction. Using such an estimate, we obtain $\eta_{\text{internal}}=53\%$ for the cascaded structure and $\eta_{\text{internal}}=6\%$ for the single stage structure, which again reflects a nine times improvement in current efficiency in the cascaded compared to the single stage structure.

The inset to Fig. 3 shows spectrally resolved electroluminescence from the cascaded and single stage devices at the nominal LED operational output level, which had peak (cut-off) emission wavelengths of $2.39 \mu\text{m}$ ($2.51 \mu\text{m}$) and $2.45 \mu\text{m}$ ($2.59 \mu\text{m}$), respectively. Both had bandwidths covering the wavelengths of the important combination wavelength range. Though the active regions of both devices were grown with exactly the same quaternary material, the single stage device exhibited a slightly longer wavelength and slightly larger bandwidth. It has been suggested previously⁸ that the long-wavelength tail of the emission of single stage devices is extended due spatially indirect, type-II emission at the quaternary/ n -GaSb interface. In the cascaded device, relative emission from the quaternary/ n -GaSb interface should be reduced due to the emission from four other emission regions without such an interface.

Tunnel junctions are useful compared to stacked diodes soldered together only if the junctions have low series resis-

tance and do not add significant absorption. The tunnel junctions in the devices here do not add any measurable series resistance to the cascaded device. Device series resistance was determined from the differential resistance of the devices under large forward biases where diode resistance is negligible. The I - V curves in Fig. 4 for both the single and cascaded devices show identical series resistances of about $2.5 \pm 0.3 \Omega$, which is dominated by the resistance of the probe station. Within uncertainty, the tunnel junctions add no measurable series resistance. As suggested by the higher power output of the cascaded compared to the single stage LED in Fig. 3, free carrier absorption in the heavily doped but thin (100 nm) tunnel junctions is not significant. This conclusion is supported by an estimate of free carrier absorption at these wavelengths in the tunnel junctions by a Drude model, assuming a vertical emission geometry.

By cascading the quaternary active regions of double heterostructure LEDs, we have fabricated LEDs that operate with better current efficiency compared to single stage devices. Tunnel junctions in the cascaded device do not add measurable series resistance, power dissipation, or heating compared to the single stage device. For a given output power, the cascaded device operates at higher voltages (2.1 V) than the single stage device (0.7 V) but lower total current (13 vs 114 mA, or $\eta_{\text{internal}}=53\%$ vs $\eta_{\text{internal}}=6\%$ for cascaded and single stage, respectively). The total input power of the cascaded device is 26 mW compared with 80 mW for the single-stage device. Devices operate at room temperature and under continuous wave.

This research was supported in part by grants from the National Institute of Diabetes and Digestive and Kidney Diseases of the National Institutes of Health (DK-60657 and DK-02925).

- ¹J. W. Hall and A. Pollard, *Ann. Clin. Biochem.* **26**, 483 (1993).
- ²A. K. Amerov, J. Chen, and M. A. Arnold, *Appl. Spectrosc.* **58**, 1195 (2004).
- ³B. L. Carter, E. Shaw, J. T. Olesberg, W. K. Chan, T. C. Hasenberg, and M. E. Flatté, *Electron. Lett.* **36**, 1301 (2000).
- ⁴M. H. M. Reddy, J. T. Olesberg, C. Cao, and J. P. Prineas, *Semicond. Sci. Technol.* **21**, 267 (2006).
- ⁵J. T. Olesberg, C. Cao, J. Yager, J. P. Prineas, C. Coretsopoulos, M. A. Arnold, L. J. Olafsen, and M. Santillie, *Proc. SPIE*, **6094** 609403 (2006).
- ⁶J. T. Olesberg, M. A. Arnold, C. Mermelstein, J. Schmitz, and J. Wagner, *Appl. Spectrosc.* **59**, 1480 (2005).
- ⁷L. M. Dolginov, L. V. Druzhinina, M. G. Milvidskii, P. G. Eliseev, M. G. Milvidsky, V. A. Skriptkin, and B. N. Sverdlov, *Izmer. Tekh.* **6**, 65 (1981).
- ⁸For a review and references, see T. N. Danilova, B. E. Zhurtanov, A. N. Imenkov, and Yu. P. Yakovlev, *Fiz. Tekh. Poluprovodn. (S.-Peterburg)* **39**, 1281 (2005) [*Semiconductors* **39**, 1235 (2005)].
- ⁹J. P. van der Ziel and W. T. Tsang, *Appl. Phys. Lett.* **41**, 499 (1982).
- ¹⁰J. Ch. Garcia, E. Rosencher, Ph. Collot, N. Laurent, J. L. Guyaux, B. Vinter, and J. Nagle, *Appl. Phys. Lett.* **71**, 3752 (1997).
- ¹¹X. Gua, G. D. Shen, G. H. Wang, W. J. Zhu, G. Ao, and D. S. Zou, *Appl. Phys. Lett.* **79**, 2985 (2001).
- ¹²J. K. Kim, E. Hall, O. Sjölund, and L. A. Coldren, *Appl. Phys. Lett.* **74**, 3251 (1999).
- ¹³R. Q. Yang and Y. Qiu, *J. Appl. Phys.* **94**, 7370 (2003).
- ¹⁴R. Q. Yang, *Superlattices Microstruct.* **17**, 77 (1995).
- ¹⁵Chih-Hsiang Lin, Rui Q. Yang, D. Zhang, S. J. Murry, S. S. Pei, A. A. Allerman, and S. R. Kurtz, *Electron. Lett.* **33**, 598 (1997).
- ¹⁶R. Q. Yang, C. J. Hill, and B. H. Yang, *Appl. Phys. Lett.* **87**, 151109 (2005).
- ¹⁷A. A. Popov, V. V. Sherstnev, and Yu. P. Yakovlev, *Tech. Phys. Lett.* **23**, 701 (1997).
- ¹⁸I. Vurgaftman, J. R. Meyer, and L. R. Ram-Mohan, *J. Appl. Phys.* **89**, 5815 (2001).